Limnol. Oceanogr., 38(2), 1993, 372–381

Theoretical analysis of size distributions determined with screens and filters

Bruce E. Logan
Environmental Engineering Program, Department of Civil Engineering and Engineering Mechanics, University of Arizona, Tucson 85721

Abstract

Nets, screens, and filters are used to sieve out particles larger than the pore sizes. However, during separation a significant fraction of particles smaller than the pore diameters will also be removed by collision and adhesion to the mesh fibers. Two filtration models were used to predict the size and mass distributions of particles during size separation. A capillary tube model was used to calculate particle removal by different screens, and a fibrous filter model was used for glass-fiber filters. The extent of particle removal was modeled assuming a size distribution of 3,100 particles evenly distributed at logarithmic intervals over 31 size classes ranging from 0.1 to 100 μm. As many as 8% of the particles and 50% of the total particle mass could be retained by a 210-μm (pore diam) mesh even though all particles were <100 μm. This high retention of particles implies that when size distributions are prepared with screens and filters, the mass concentration in smaller size fractions will be considerably underestimated.

Screens and filters are routinely used by aquatic scientists to separate and concentrate material (e.g. Mullin 1965; Malone 1971). By passing water samples through a series of screens, samples can be separated into different size distributions and further analyzed. For example, Back et al. (1991) size-fractionated lake-water samples through 53- and 10-μm Nitex nets and determined the distribution of Chl *a* and other photosynthetic parameters. Similarly, Azam and Hodson (1977) used different pore-diameter Nuclepore and Millipore filters to separate marine bacteria according to size.

A body of literature on filtration has been developed to predict removal of colloidal aerosol particles by filters, but these models have not been applied to size fractionation of aquatic samples with screens and filters. Two different approaches have been used to construct these models. The first considers the filter to be a bundle of fibers (e.g. models by Fuchs 1964; Hinds 1983). The second model is based on flow through small capillary tubes or pores (Pich 1966; Spurney et al. 1969). Of these two models, only the fibrous models have been used to predict aquasol removal in marine systems by a variety of organisms including echinoderm larvae, brittle stars, bdelloid rotifers, sea anemones, and zoanthids (Rubenstein and Koehl 1977). Recently, fiber models have been applied to grazing by cladocerans and the removal of particles on nets spun by caddisfly larvae (Fuller et al. 1983; Loudon 1990; Brendelberger 1991).

A comparison of the fiber and capillary pore models by Rubow and Liu (1986) showed that the fibrous models could be used to predict aerosol removal by fibrous filters and that only the pore models successfully predicted aerosol removal by Nuclepore filters. Further experiments have shown that fibrous models are also applicable to aquasol removal by glass-fiber and other types of large-pore fibrous filters (Logan et al. 1993). Both filtration models predict that some particles smaller than the mesh pore diameter will be retained by the net, in agreement with experimental observations. For example, studies on particle capture by the rectangular nets made by caddisfly larvae have shown that a substantial fraction of particles smaller than the net pores are retained, and the net removal efficiency is a function of the size and nature of the particle captured (Fuller et al. 1983; Loudon 1990). Malone et al. (1979) determined that 50% of material with a mean diameter of 16 μm was removed by mesh with a 22-μm more diameter.

The removal of particles smaller than mesh pores can result in a distribution of particle sizes retained on the net that does not reflect

Acknowledgments

I thank Mark Gross for performing the filtration experiments and calculating microsphere sticking coefficients.

Funding was provided by ONR grant N00014-91-J-1249, National Institutes of Environmental Health Sciences grant P42ES04940, and NSF equipment grant BCS 90-08145.

the size distribution of particles in the water column. Sheldon (1972) compared particle removal by cellulose (Millipore) and glass-fiber (Whatman) filters with particle removal by polycarbonate (Nuclepore) filters. He found that polycarbonate filters produced the sharpest separation of particles into size classes smaller than the nominal pore size. Glass-fiber and cellulose filters removed particles over a much wider size interval and were not recommended for separating particles by size.

The effect of screens and filters on measured particle size distributions can be determined with filtration models, but only if appropriate models are used. Although the capillary pore model can be used to predict particle removal by Nuclepore filters, this model has not been applied to particle removal in aqueous systems. Here it is argued that capillary pore models should be used to calculate particle removal by screens and polycarbonate filters, and fiber models should be used for glass-fiber, cellulose, and other fibrous filters. These two models can be used to determine whether samples should be collected in series or in parallel and to determine appropriate sizes of screens and mesh for sampling and separating particles into different size distributions. Fluorescent microspheres are used as model destabilized particles, providing estimates of collision efficiencies of particles with screen surfaces.

Methods

Particle retention by screens—The retention of particles by uniformly sized screens was evaluated with fluorescently labeled carboxylate microspheres (type YG Fluoresbrite, Polysciences Inc.) ranging in diameter from 0.49 to 4.12 μm. Microspheres were chosen because they are available in precise sizes and shapes and, unlike microorganisms, would not change chemical surface properties during experiments. Screens used in experiments (Spectramesh) or in model calculations had pore diameters ranging from 10 to 1,000 μm (Table 1) and were made of nylon, polypropylene, or polyethylene. Circular pieces of screens (2.4-cm diam) were cut from large sheets and placed in a 10-place vacuum manifold box containing stainless steel funnels and bases, and Teflon valves (Hoefer Sci.). The screen was covered by a Teflon gasket held in place by the heavy funnel to prevent leakage around the edges of the screen.

Table 1. Physical characteristics of screens and filters used in calculations.

Code	Material	Diameter (μm)		
		Pore	Fiber	Porosity
NY10	Nylon	10	45	0.05
NY20	Nylon	20	55	0.14
NY30	Nylon	30	70	0.21
NY60	Nylon	60	55	0.45
PP210	Polypropylene	210	320	0.34
PE230	Polyethylene	230	280	0.42
PP1000	Polypropylene	1,000	1,020	0.45
GF/C	Glass fiber	4.1	2.2	0.89

Microspheres were suspended in a phosphate buffer (0.5 g K_2HPO_4, 1 g NH_4Cl, 0.2 g $MgSO_4 \cdot 7H_3O$, 0.4 mg $FeCl_3$ per liter of ultrapure water), sonicated 20–25 min to break up any aggregates, and examined at 400 and 1,000× with a microscope to verify that no aggregates were present in the sample. Screens were rinsed with 5 ml of buffer before and after addition of bead solution. Fluid containing microspheres ($\sim 10^6$ ml^{-1}) was pipetted (10 ml) into the funnel, gravity filtered through the screens, and slowed to ensure laminar flow through the mesh. All measurements were made in duplicate. The number of particles retained on the mesh was estimated by illuminating the screens with UV light and counting 15–20 fields at 1,000× with epifluorescence microscopy (BH2, Olympus).

Fiber filtration model—Most fiber filtration models were originally developed to predict aerosol particle removal by fibrous filters. These models were later adapted by others (Yao et al. 1971; Rubenstein and Koehl 1977; Silvester 1983) to describe particle removal in aqueous systems. According to the fiber model, the reduction in particle concentration after flow through a filter of length L at steady state (Yao et al. 1971) is

$$\frac{C}{C_0} = \exp\left(-\xi\alpha\phi\eta\frac{L}{d_c}\right) \quad (1)$$

where C_0 and C are the aquasol concentrations entering and leaving a filter, ξ is a geometric factor equal to 3/2 for spherical and $4/\pi$ for cylindrical collectors of diameter d_c, α a collision or sticking efficiency of the particle with the collector, $\phi = (1 - p)$ the solid fraction, p

the filter-bed porosity, and η the collector collision efficiency which is a function of filter geometry and fluid hydrodynamics. Equation 1 was developed from a mass balance around an isolated collector. For flow in a packed bed, the porosity term ϕ should be divided by the filter porosity (Flagan and Seinfeld 1988). For filtration by high-porosity filters this correction is small and will be neglected in the calculations presented below.

The collector efficiency is the sum of the single-collector efficiencies describing particle removal of size d_p due to diffusion (η_D), interception (η_I), and gravity (η_G). For spherical collectors, Yao et al. (1971) used

$$\eta_D = 4\mathrm{Pe}^{-\frac{2}{3}}, \tag{2}$$

$$\eta_I = \frac{3}{2}R_c^2, \tag{3}$$

and

$$\eta_G = G. \tag{4}$$

Collector efficiencies are dimensionless and are developed from correlations involving three dimensionless numbers: the Peclet number $\mathrm{Pe} = U_0 d_c/D$, the interception number $R_c = d_p/d_c$, and the gravitational number, $G = U_p/U_0$, where U_0 and U_p are the filter superficial velocity and particle settling velocity, and D is the particle diffusivity. The particle settling velocity is obtained from Stokes' law, or

$$U_p = \frac{g(\rho_p - \rho_f)d_p^2}{18\mu} \tag{5}$$

where ρ_p and ρ_f are the particle and fluid densities, g the gravitational constant, and μ the fluid dynamic viscosity. The particle diffusivity is obtained from the Stokes-Einstein equation as

$$D = \frac{kT}{3\pi\mu d_p} \tag{6}$$

where k is Boltzman's constant (1.38×10^{-23} J K^{-1}) and T the absolute temperature.

The Yao model was shown to provide reasonable agreement with data on removal of latex beads in packed-bed columns (Yao et al. 1971), but the model is known to underestimate the number of particle collisions with filter material in packed-bed columns. Underestimation of collisions can produce sticking coefficients greater than unity (Logan et al. 1993). Several other filtration models have been developed that predict increased particle collisions (e.g. Rajagopalan and Tien 1976; Rubow and Liu 1986). These models use empirical equations developed for specific filtration conditions such as packed beds of spheres or aerosol filtration and produce lower calculated sticking coefficients. Since these models all predict the same general removal patterns with particle size, and since sticking coefficients for particles in filters using the Yao model are typically less than unity for particles in filters (Logan et al. 1993), the Yao model is used here.

Capillary tube model—Capillary tube models are based on the assumption that filters consist of a series of tubes. These models were shown by Spurny et al. (1969) to accurately predict aerosol removal by Nuclepore filters. The overall filter efficiency is the sum of removal by individual mechanisms minus the removal that occurs by mechanism overlap, or

$$E_T = \alpha\,(\eta_{Dc} + \eta_{Rc} + \eta_{Ic} - \eta_{Dc}\eta_{Rc} - \eta_{Rc}\eta_{Ic} - \eta_{Dc}\eta_{Ic} + \eta_{Dc}\eta_{Rc}\eta_{Ic}) \tag{7}$$

where η_{Dc}, η_{Rc}, and η_{Ic} are the individual removal mechanisms for diffusion, interception, and impaction based on the capillary tube model. Particle removal by impaction into the filter surface is important for dense particles in air, but is relatively unimportant for particle removal in aqueous solutions where particle and fluid densities are similar. For aquasols, Eq. 7 becomes

$$E_T = \alpha(\eta_{Dc} + \eta_{Rc} - \eta_{Dc}\eta_{Rc}). \tag{8}$$

For diffusion, removal is calculated (Rubow and Liu 1986) with

$$\eta_{Dc} = 2.56D_c^{\frac{2}{3}} - 1.2D_c - 0.177D_c^{\frac{4}{3}} \tag{9}$$

where D_c is a dimensionless number defined as

$$D_c = \frac{4LDp}{d_h^2 U_0}, \tag{10}$$

and d_h is the pore diameter. Equation 9 is only valid for $D_c < 0.001$, which is within the range of values used here.

Particles are removed by interception when the fluid streamlines bring a particle sufficiently close to the pore surface. Removal by interception is calculated (John et al. 1978) with

$$\eta_{Rc} = (2R_h - R_h^2)^{\frac{3}{2}} \tag{11}$$

where $R_h = d_p/d_h$ is the interception number

based on pore diameter. Equation 11 has been shown to provide good agreement with experimental work on aerosol removal in Nuclepore filters (Rubow and Liu 1986).

Size and mass distributions—The calculations made below are based on a discrete size distribution consisting of 3,100 particles separated into 31 size classes ranging from 0.1 to 100 μm. Each particle class is separated in size by 0.1 log units [$d_i = 10^{(-1+0.1i)}$, $i = 0$–30] and contains 100 particles of size d_i. All particles are assumed to be spheres with a mass m_i calculated from the volume with $m_i = (\pi/6)d_i^3$.

Size separations are determined based on the geometry of commercially available screens (Spectramesh Co.) with pore sizes and mesh surface areas as specified by the manufacturer (Table 1). For my calculations on particle removal by screens, it is assumed that the pore length is equal to the mesh-fiber diameter. The fiber size (2.2 μm), pore diameter (4.1 μm), and filter depth (300 μm) for glass-fiber filters (GF/C, Whatman Co.) are those used by Logan et al. (1993) to model bacteria and particle removal by filters. In example calculations, the following are used: $U_0 = 0.088$ cm s^{-1}, $\mu = 0.01$ g cm^{-1} s^{-1}, $\rho_p = 1.05$ g cm^{-3}, $T = 293$ K, and (unless indicated otherwise) $\alpha = 1$.

Results

Comparison of fiber and pore models—Both the fiber and pore models predicted that a wide range of particle sizes would be removed by a 30-μm pore-diameter mesh and that a large fraction of these particles would be smaller than the pore diameter (Fig. 1). The pore model indicates that a larger number of particles of a given size would be removed by the mesh than indicated by the fiber model. For example, the size of a particle that is 10% removed by mesh with a 30-μm pore diameter is 10 μm ($d_{10} = 10$ μm) for the fiber model, although the pore model predicts 50% removal for this size particle ($d_{50} = 10$ μm); for the pore model, $d_{10} = 3$ μm.

The fiber model predicts that 60% of particles with a diameter equal to the pore diameter ($d_{40} = 30$ μm) will not be removed and that 20% of particles 60 μm in diameter, or twice the size of the pore, would pass through the mesh. The fiber model is based on the probability of particle capture by a number of collectors and is not directly a function of pore diameter (*see Eq. 1–6*). As a result, the fiber model allows for the possibility that particles larger than the pore diameter of the mesh will pass through the mesh. Because this is impossible, the fiber model should not be used to model particle removal by screen filters, which consist of only a single collector.

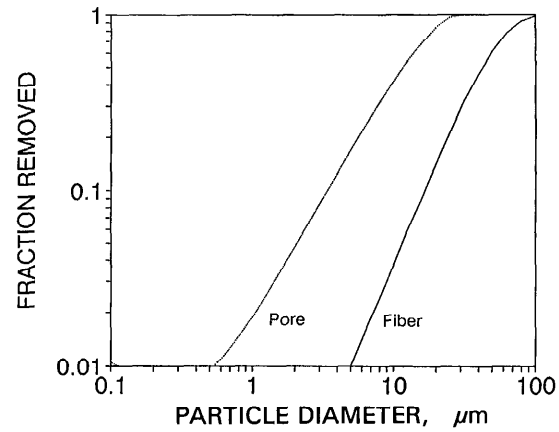

Fig. 1. Predicted fraction of particles removed with the pore and fiber models for a 30-μm pore-diameter screen (NY30). Note that the fiber model predicts some particles larger than the pore will pass through the mesh.

Retention of microspheres on screens—The retention of six sizes of beads in 10, 20, and 30-μm pore-diameter mesh ranged from 0.26 to 8.2% (Fig. 2). The fraction of particles retained was variable but spanned the predicted values. The average sticking coefficients, calculated with the pore model for the 10-, 20-, and 30-μm pore-diameter mesh, are shown in Table 2. Sticking coefficients for microspheres on 210-μm pore-diameter polyproplyene screens were slightly lower than those for 230-μm polyethylene screens (Table 2).

The sticking coefficient α is calculated as the unknown in the filtration models, so variation in α reflects model bias. In general, values of α varied from 0.1 to 1 for the smaller beads (≤ 1 μm), while larger beads had values of α closer to 0.1 (Fig. 3). Lower sticking coefficients for smaller beads suggest that the model is underestimating collision frequencies of smaller sized particles. Unless otherwise indicated, it is assumed in the calculations below that particles are completely destabilized, i.e., that $\alpha = 1$. The assumption that $\alpha = 1$ results in the maximum predicted particle removal and provides an upper limit in the calculated particle retention by filters and screens.

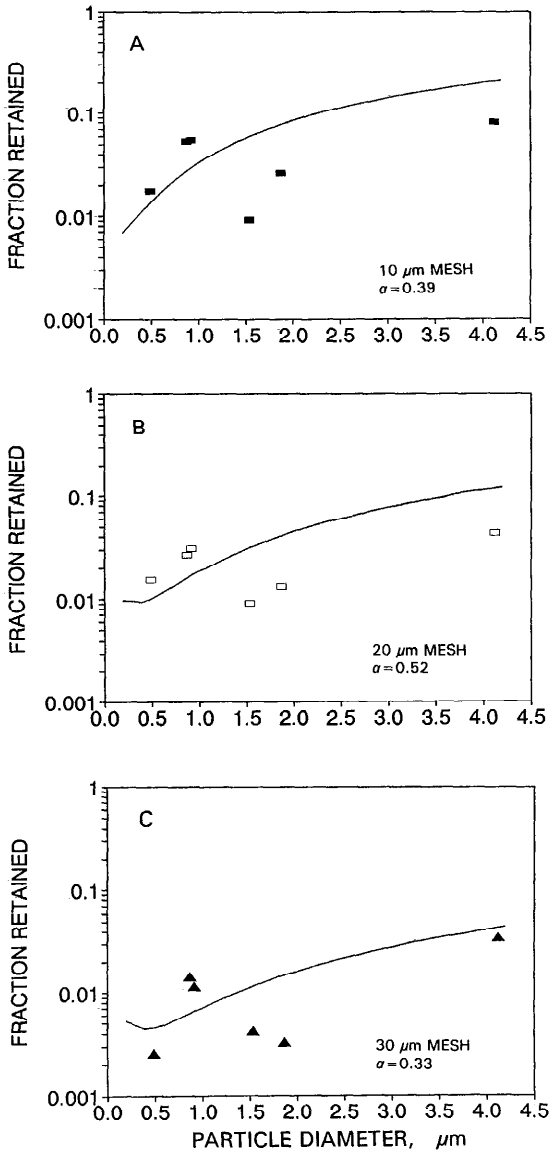

Fig. 2. Observed and predicted fraction of microspheres removed on 10-, 20-, and 30-μm pore-diameter nylon screens.

Mechanisms of particle removal—The primary mechanism of particle removal, calculated with the capillary tube model for all screens, is interception. For a 230-μm pore-diameter mesh, essentially all particles >3 μm are removed by interception (Fig. 4A). Particles <0.2 μm are primarily removed by diffusion. The dominant mechanism of particle removal is interception, since for all screens

Table 2. Esitmates of sticking coefficients (α) for microspheres calculated with capillary pore model.

Particle sizes (μm)	Mesh material	Mesh pore diam (μm)	α*	n
0.49–4.19	Nylon	10	0.39±0.12	6
0.49–4.19	Nylon	20	0.52±0.15	6
0.49–4.19	Nylon	30	0.33±0.10	6
0.5–2.2	Polypropylene	210	0.33±0.68	3
0.5–2.2	Polyethylene	230	0.50±0.97	3

* ± SE; in parentheses—number of bead sizes examined (in duplicate).

examined interception is the only mechanism that accounts for removal of >1% of particles in a size category.

The fiber model is known to adequately describe particle removal by glass-fiber (GF/C) filters (Logan et al. 1993). Particles larger than the pore diameter will be sieved out on the filter surface, while smaller particles will be removed within the filter by collisions with fibers. Over a range of 0.1–1 μm, both diffusion and interception mechanisms contribute to particle removal (Fig. 4B). Particles <0.1 μm would be removed primarily by diffusion.

Removal efficiency—The fraction of particles removed when a sample is passed, in parallel, through three different mesh sizes (30, 230, and 1,000 μm) and a glass-fiber filter (GF/C) is shown in Fig. 5. Although the 1,000-μm pore is 10 times as large as the largest particle (100 μm), 1–10% of particles 25–100 μm in diameter are removed by the mesh. Particle removal by smaller mesh exhibit a similar pattern of removal for particles smaller than the mesh pores. The glass-fiber filter contains many

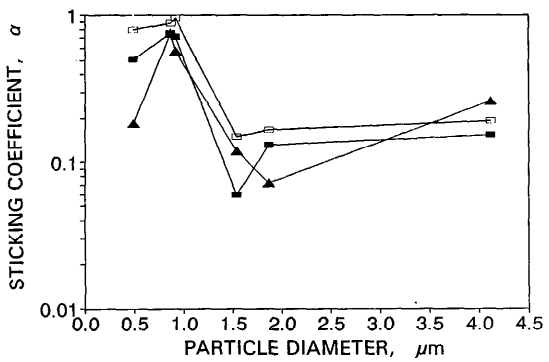

Fig. 3. Variation in sticking coefficient with microsphere diameter for the nylon screens with pore diameters of 10 (■), 20 (□), and 30 (▲).

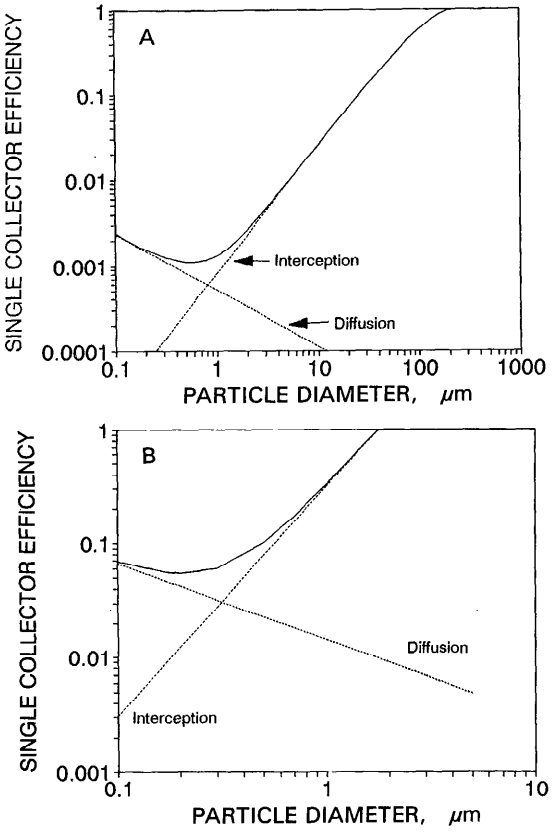

Fig. 4. Single collector efficiencies (dashed lines, diffusion and interception) and total efficiency (solid lines) calculated with (A) the pore model for 230-μm-pore-diameter mesh (PE230) and (B) the fiber model for a glass-fiber filter (GF/C).

layers of fibers and effectively removes particles <1 μm. The median particle passing through the glass-fiber filter is in the range of 0.2–0.3 μm in diameter.

Parallel vs. serial processing—The efficiency of mesh and filters is also commonly evaluated in terms of percent penetration, where penetration P, calculated as $P = (1 - E) \times 100$, reflects the ability of mesh and filters to pass particles. The penetration of particles through two mesh sizes (30 and 230 μm) and one filter (GF/C) is shown in Fig. 6 for samples processed in parallel and in series. The samples prepared in series were assumed to have been prescreened with a 1,000-μm mesh (PP1000). There is a decrease of <3% in the overall penetration of particles through the 230-μm mesh when samples are processed in series. Because

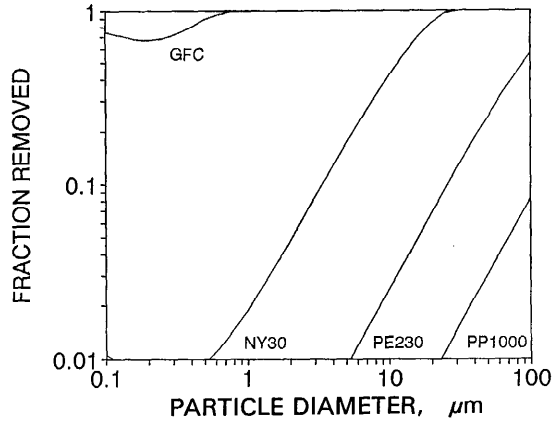

Fig. 5. The fraction of particles removed by three screens and a glass-fiber filter for a sample processed in parallel.

there is little overlap in sizes of particles removed by these screens (*see Fig. 5*), this result is expected. The differences in particle size distributions obtained by serial and parallel processing would be important only for screens with very similar pore sizes. Therefore, the major effect on the overall penetration, and the resulting size distribution, should be the size of the mesh and not how the sample is processed.

Size distributions—The effect of removal of particles smaller than the mesh pores is a reduction of mass in the actual size categories. When the sample is passed (in parallel) through 1,000-, 230-, and 30-μm-diameter mesh and

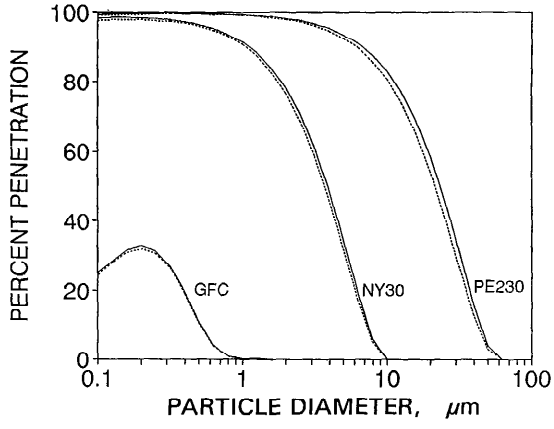

Fig. 6. Comparison between processing samples in parallel (solid lines) and series (dashed lines) with three screens (PP1000, not shown) and a glass-fiber filter.

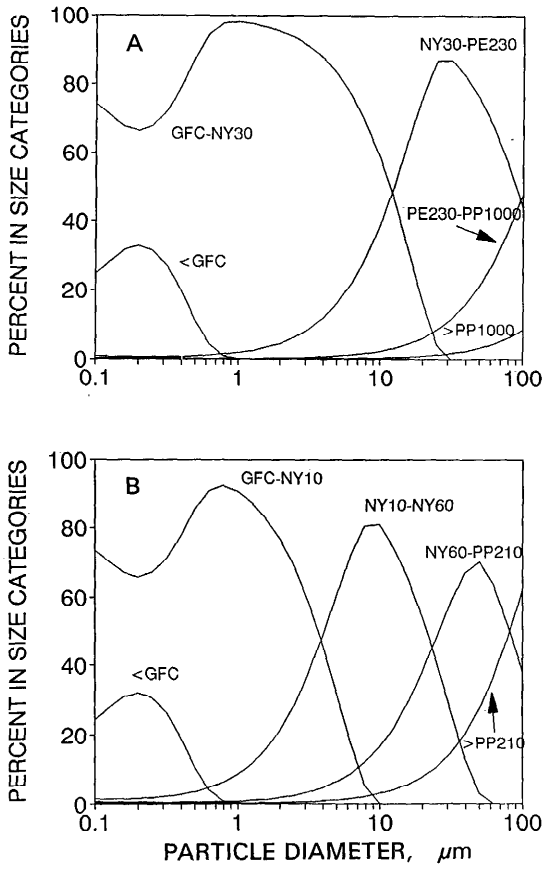

Fig. 7. Number of particles calculated to be in different size distributions from serial processing of a sample through screens (A: PP1000, PE230, NY30; B: PP210, NY60, NY10) and a glass-fiber filter. Table 3 summarizes actual and calculated number distributions.

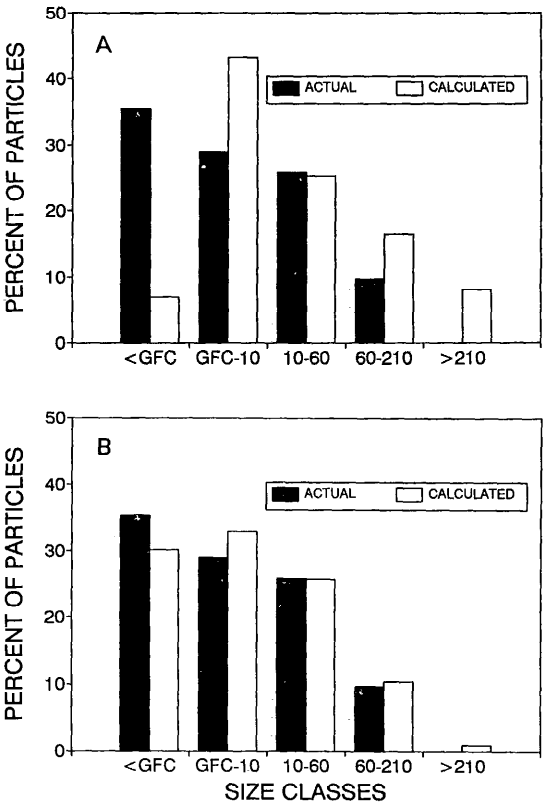

Fig. 8. Calculated vs. actual percent of particles (by number) in size classes after separation with 210-, 60-, and 10-μm pore-diameter mesh and a glass-fiber filter, assuming sticking coefficients of (A) 1.0 and (B) 0.1.

a glass-fiber filter, the calculated size distributions are much broader than the actual distributions (Fig. 7A). A separation with screens with a narrower separation of pore diameters (Fig. 7B using 210-, 60-, and 10-μm screens) and a GF/C filter results in <90% of particles in any size class contributing to the actual size class.

The major effect on the size distribution occurs from removal of smaller particles by mesh with the largest pore diameter (Fig. 8A). For example, 60% of particles with a diameter of 100 μm could be removed by a 210-μm mesh. When all other particles in the size distribution are included, 8% of the total number of particles and 50% of the total particle mass could be removed by a mesh with a pore diameter larger than any of the particles in the system (Table 3). The difference between the calculated numbers of particles and the actual numbers of particles is 171% for the 60–210-μm size class, 98% for the 10–60-μm size class, and 149% for the particles larger than the nominal pore of the GF/C filter (4.7 μm) and a 10-μm mesh (Table 3).

Because the largest particles have the most mass, the errors in the mass distribution are substantial. The 210-μm mesh is calculated to retain 50.1% of the total mass of particles even though none of the particles in the size distribution exceed 100 μm. Errors in mass for the other size distributions range from 3 to 54.6%, although some of the mass in these size distributions are due to particles smaller than the pore diameters.

The measured size distributions become more accurate as the sticking coefficient de-

Table 3. Particle size distributions based on number and mass concentrations.

Mesh pore diam (μm)	% of particles (by number)			% of particles (by mass)		
	Calc.	Actual	Diff.*	Calc.	Actual	Diff.*
>210	8.0	0.0	—†	50.1	0.0	—†
60–210	16.6	9.7	171	47.7	87.4	55
10–60	25.2	25.8	98	2.2	12.5	17
GF/C–10	43.4	29.0	149	9.9×10^{-3}	5.0×10^{-2}	20
<GF/C	6.9	35.5	19	3.0×10^{-6}	1.0×10^{-4}	3

* Determined as 100 × (C/A), where C and A are the calculated and actual amount of particles (number or mass) in the size classes indicated.
† Could not be determined because actual = 0.

creases because the screens begin to act more like sieves than filters. When $\alpha = 0.1$, for example, only 5% of the mass is retained on a 210-μm screen (Fig. 8B). The glass-fiber filter has a large number of collectors and removes the most particles larger than the nominal pore diameter. Therefore, screens will begin to function more like sieves than filters as particle adhesion to the screen material decreases. The extent that particle numbers and mass in smaller size classes of size distributions are underestimated will be a direct function of particle sizes and sticking coefficients.

Discussion

Filtration efficiencies of screens composed of rectangular mesh should not be calculated with models based on bundles of fibers for several reasons. Fiber models are based on the probability of particle capture by a number of collectors. Because the pore diameter is not directly used in the removal equation (i.e. Eq. 1), the fiber model allows for the possibility of particles larger than the pore diameter of the mesh passing through it. In the case of typical mesh used for size fractionation, I found that the fiber model predicted particles larger than the mesh pore diameter could pass through the filter. In contrast, all particles larger than the pore diameter were predicted to be removed with the capillary pore model (Fig. 1). On this basis alone, the capillary pore model is more useful for estimating particle removal by screens. In addition, most screens used to separate particles have a high fraction of surface area and regularly shaped pores that more closely resemble the morphology of Nuclepore filters than fibrous filters. For aerosol particles, capillary pore models have been shown to be more accurate than fiber models in predicting particle removal by polycarbonate (Nuclepore) filters. It is reasonable, therefore, that capillary pore models also predict aquasol particle removal by screens more accurately than fiber models.

Several calculations were made to determine the effects of size separation by a series of screens with different pore diameters. Although these screens sieve particles larger than the pore diameter, a large fraction of the total mass smaller than the pore diameter can be removed by the mesh when particles have large sticking coefficients ($\alpha = 1$). For example, 8% of the particles and 50% of the particle mass in a size distribution spanning a range of 0.1–100 μm were predicted to be removed by a 210-m pore-diameter mesh (Table 3). For a 30-μm mesh, >50% of particles >10 μm would be removed. As a result, the average size of a particle removed by a screen is overestimated by the manufacturer's pore diameter. These calculations are in agreement with experimental results demonstrating that separations do not produce discrete size distributions (Sheldon 1972; Malone et al. 1979; Runge and Ohman 1982).

Similar effects on the size and mass distributions of particles were found for particle removal by a glass-fiber (GF/C) filter. Although 35.5% of the particles were smaller than the nominal pore size of the filter (4.7 μm), only 6.9% of the mass was calculated (with a fiber model) to pass through the filter. The median-sized particle that penetrated the filter was in the range of 0.2–0.3 μm, over an order-of-magnitude smaller than the nominal pore diameter.

One additional factor that will affect the size separation, not included in the above discussion, is filter clogging. As large amounts of material are deposited on net and filter fibers, pore sizes will decrease and fiber diameters will in-

Table 4. Estimates of sticking coefficients (α) calculated with the fiber model.

Particle type	Particle size (μm)	Test conditions	α	Reference
Microspheres	0.9–26	Column (glass)	>1.0	Yao et al. 1971
Bacteria	~1	Column (silica)	0.2	Logan et al. 1993
Microspheres	0.5	Column (silica)	1.2	Logan et al. 1993
Bacteria	~1	Filter (GF/C)	0.09–0.25	Logan et al. 1993
Microspheres	0.5	Filter (GF/C)	0.87	Logan et al. 1993

crease. Pore size reduction results in more efficient removal of increasingly smaller particles. Danielsson (1982), for example, has shown that clogging of fibrous filters resulted in the removal of dissolved and colloidal Fe in a water sample. A recent review by Buffle et al. (1992) addresses several experimental problems in obtaining accurate size separations. They emphasize that it is extremely important to stop filtering a sample *before* the filter has clogged, as evidenced by a decrease in filtration flow rate. Particles smaller than the pore diameter can be removed at the surfaces of polycarbonate filters through "surface coagulation" or the production of large aggregates due to pore clogging. Buffle et al. recommend that low filtration velocities be used to minimize coagulation and that filters not be reused.

In most calculations, it was assumed that sticking coefficients for all particles were unity. However, it is expected that the magnitude of the sticking coefficients will vary depending on the mesh material, the type of particle (i.e. algae, bacteria, inorganic colloids, etc.), and solution characteristics such as ionic strength and concentration of organic molecules. Several experiments have been conducted to determine a reasonable range of particle sticking coefficients. Yao et al. (1971) tested their filtration model with carboxylate microspheres and a column packed with glass beads (500-μm diam). Based on their experiments, it was estimated that sticking coefficients increased from $\alpha = 0.44$ to values greater than unity ($1.8 \leq \alpha \leq 5.0$) when a polymer coagulant was added to their column before filtration (Logan et al. 1993). Similar experiments with silica beads (500 μm) and no coagulant have been found to produce sticking coefficients of ~1.2 for microspheres and 0.2 for bacteria (Table 4).

Sticking coefficients have also been calculated with the fiber model for particles vacuum filtered through glass-fiber (GF/C) filters (Logan et al. 1993). In those experiments it was calculated that $\alpha = 0.87$ for fluorescent microspheres and $0.09 \leq \alpha \leq 0.25$ for several pure cultures of laboratory-grown bacteria (Table 4).

I am currently conducting experiments with others (Logan et al. unpubl. data) to measure the sticking coefficients of several species of laboratory-grown phytoplankton. Preliminary results indicate sticking coefficients of 0.2–0.5 for *Nitzschia angularis* ($d_p = 17$ μm) and 0.3–1 for *Chaetoceros gracilis* ($d_p = 7$ μm) during exponential growth. These sticking coefficients may be a function of growth phase because sticking coefficients increase as cultures enter late-log and stationary growth. However, this observation may also be a result of flocculation, resulting in the formation of particles larger than the assumed primary particle size. In related experiments Kiørboe et al. (1990) have shown that phytoplankton sticking coefficients, derived from coagulation experiments (i.e. cell-cell attachment), can change by several orders of magnitude during a batch growth cycle.

The above studies suggest that sticking coefficients for many different particles separated by nets, screens, and glass-fiber filters are in the range of 0.1 to unity. The magnitude of the sticking coefficient shifts the removals calculated in Eq. 1 and 10 by different amounts. For the pore model, retention is directly reduced in proportion to the sticking coefficient (Eq. 10). For the fiber model, retention decreases proportional to exp $(-\alpha)$ (Eq. 1). In this range of sticking coefficients (0.1–1), fibrous filters were not calculated to produce accurate size distributions, in agreement with experimental studies on marine particles (Sheldon 1972).

Size distributions calculated for samples separated by screens indicate that screening

produces reasonably accurate size distributions when sticking coefficients are ≤ 0.1 (Fig. 8B). Screens are useful for providing approximate size distributions, however, the actual size distribution will be a function of the screen sizes and materials used. Changes in particle adhesion, caused by changes in surfaces of particles and the concentrations or types of dissolved materials, can alter particle retention by nets. These changes could result in an apparent change in a size distribution, when the only real change may have been a change in the adhesion of the particles for the screening material.

References

AZAM, F., AND R. E. HODSON. 1977. Size distribution and activity of marine microheterotrophs. Limnol. Oceanogr. **22:** 492–501.

BACK, R. C., D. W. BOLGRIEN, N. E. GUSELNIKOVA, AND N. A. GONDARENKO. 1991. Phytoplankton photosynthesis in southern Lake Baikal: Size-fractionated chlorophyll *a* and photosynthetic parameters. J. Great Lakes Res. **17:** 194–202.

BRENDELBERGER, H. 1991. Filter mesh size of cladocerans predicts retention efficiency for bacteria. Limnol. Oceanogr. **36:** 884–894.

BUFFLE, J., D. PERRET, AND M. NEWMAN. 1992. The use of filtration and ultrafiltration for size fractionation of aquatic particles, colloids and macromolecules, p. 171–230. *In* J. Buffle and H. P. van Leeuwen [eds.], Environmental particles. Lewis.

DANIELSSON, L. G. 1982. On the use of filters for distinguishing between dissolved and particulate fractions in natural waters. Limnol. Oceanogr. **16:** 179–182.

FLAGAN R. C., AND J. H. SEINFELD. 1988. Fundamentals of air pollution engineering. Prentice-Hall.

FUCHS, N. A. 1964. The mechanics of aerosols. Pergamon.

FULLER, R. L., R. J. MACKAY, AND H. B. N. HYNES. 1983. Seston capture by *Hydropsyche betteni* nets (Trichoptera; hydropsychidae). Arch. Hydrobiol. **97:** 251–261.

HINDS, W. C. 1983. Aerosol technology. Wiley.

JOHN, W., G. REISCHL, S. GOREN, AND D. PLOTKIN. 1978. Anomolous filtration of solid particles by Nuclepore filters. Atmos. Environ. **12:** 1555–1557.

KIØRBOE, T., K. P. ANDERSEN, AND H. G. DAM. 1990. Coagulation efficiency and aggregate formation in marine phytoplankton. Mar. Biol. **107:** 235–246.

LOGAN, B. E., T. A. HILBERT, AND R. G. ARNOLD. 1993. Using filtration models to describe removal of bacteria in different types of laboratory filters. Water Res. **27:** In press.

LOUDON, C. 1990. Empirical test of filtration theory: Particle capture by rectangular-mesh nets. Limnol. Oceanogr. **35:** 143–148.

MALONE, T. C. 1971. The relative importance of nannoplankton and net plankton as primary producers in tropical oceanic and neritic phytoplankton communities. Limnol. Oceanogr. **16:** 633–639.

———, M. B. CHERVIN, AND D. C. BOARDMAN. 1979. Effects of 22-μm screens on size-frequency distributions of suspended particles and biomass estimates of phytoplankton size fractions. Limnol. Oceanogr. **24:** 956–960.

MULLIN, M. M. 1965. Size fractionation of particulate organic carbon in the surface waters of the western Indian Ocean. Limnol. Oceanogr. **10:** 459–462.

PICH, J. 1966. Theory of aerosol filtration by fibrous and membrane filters, p. 223–285. *In* C. N. Davies [ed.], Aerosol science, Academic.

RAJAGOPALAN, R., AND C. TIEN. 1976. Trajectory analysis of deep-bed filtration with the sphere-in-a-cell porous media model. AIChE J. **22:** 523–533.

RUBENSTEIN, D. I., AND M. A. R. KOEHL. 1977. The mechanisms of filter feeding: Some theoretical considerations. Am. Nat. **111:** 981–994.

RUBOW, K. L., AND B. Y. H. LIU. 1986. Characteristics of membrane filters for particle collection, p. 74–94. *In* Fluid filtration: Gas. V. 1. ASTM Tech. Publ. 975.

RUNGE, J. A., AND M. D. OHMAN. 1982. Size fractionation of phytoplankton as an estimate of food availability to herbivores. Limnol. Oceanogr. **27:** 570–576.

SHELDON, R. W. 1972. Size separation of marine seston by membrane and glass-fiber filters. Limnol. Oceanogr. **17:** 494–498.

SILVESTER, N. R. 1983. Some hydrodynamic aspects of filter feeding with rectangular-mesh nets. J. Theor. Biol. **103:** 265–286.

SPURNY, K. R., J. P. LODGE, JR., E. R. FRANK, AND D. C. SHEESLEY. 1969. Aerosol filtration by means of Nuclepore filters: Structural and filtration properties. Environ. Sci. Technol. **3:** 453–464.

YAO, K., M. T. HABIBIAN, AND C. R. O'MELIA. 1971. Water and wastewater filtration: Concepts and applications. Environ. Sci. Technol. **5:** 1105–1112.

Submitted: 12 March 1992
Accepted: 5 October 1992
Revised: 6 November 1992